JOURNAL OF MATERIALS SCIENCE 6 (1971) 313–318

Electron Microscopy of Lithium Ferrites. Precipitation of $LiFe_5O_8$ in α—$LiFeO_2$

J. G. ALLPRESS
Division of Tribophysics, CSIRO, University of Melbourne, Vic. 3052, Australia

α-$LiFeO_2$, which has the rocksalt structure, loses lithium when it is heated in air at temperatures above about 1000° C. The consequent non-stoichiometry is retained by rapid quenching, but slower rates of cooling are accompanied by precipitation of the ferrimagnetic spinel, $LiFe_5O_8$. The size, shape, and structure of the precipitate particles depends upon the thermal treatment of the samples.

1. Introduction

A number of examples of the precipitation of spinels from solid solutions having structures analogous to that of rocksalt have been reported in recent years [1]. These composite materials have interesting and potentially useful properties, particularly when the precipitated phase is ferrimagnetic [2]. This paper draws attention to another system of this kind, the precipitation of the ferrimagnetic spinel $LiFe_5O_8$ from α-$LiFeO_2$. Crystallographic data for these phases are given in table I. The precipitation was observed during a study of the thermal decomposition of α-$LiFeO_2$.

TABLE I Crystallographic data for the cubic phases α-$LiFeO_2$ and $LiFe_5O_8$.

Phase	Space group	a Å	Reference
α-$LiFeO_2$	Fm3m	4.157	3
$LiFe_5O_8$ disordered	Fd3m	8.330	4
$LiFe_5O_8$ ordered	$P4_332$	8.333	5

2. Experimental

Ceramic specimens of α-$LiFeO_2$ and $LiFe_5O_8$ were prepared by heating finely ground mixtures of appropriate proportions of high purity Li_2CO_3 and Fe_2O_3 at 800° C for 3 days in air. The products were then compressed into pellets and sintered at 1100° C for 2 h, in order to increase the grain size. Fracture fragments of the sintered material, prepared by grinding in an agate mortar, were distributed on carbon-coated specimen grids and examined in a Philips EM200 electron microscope. Many of the edges of the fragments were very thin and suitable for transmission diffraction and microscopy.

3. Results

3.1. Diffraction from Pure Samples

X-ray powder diffraction patterns of the samples of α-$LiFeO_2$ and $LiFe_5O_8$ were completely indexed in terms of the unit cell data quoted in table I. The $LiFe_5O_8$ as prepared showed only the reflections of the disordered form, but extra weak lines of the ordered phase were observed after annealing a sample at 600° C for several days.

Electron diffraction patterns, showing the (001), (110) and (111) sections of the reciprocal lattices, were recorded for each sample, The (001) sections are given in figs. 1a-c. Patterns from α-$LiFeO_2$ (e.g. fig. 1a) contained distinctive arrangements of diffuse scattering in addition to the strong Bragg reflections expected from the NaCl-type lattice. The diffuse intensity arises from short-range order of the Li^+ and Fe^{3+} ions, which share the cation positions in the lattice [6]. Fig. 1b shows the (001) pattern obtained from the annealed sample of $LiFe_5O_8$. Reflections of the type $h00$, $h \neq 4n$ and $0k0$, $k \neq 4n$ are disallowed by the space group $P4_332$, but they appear in fig. 1b as a consequence of multiple diffraction. A fully disordered sample of $LiFe_5O_8$ was obtained by quenching from 950° C into water [5]. Diffraction patterns from this material (e.g. fig. 1c) contained strong reflections expected for the space group Fd3m, and very faint diffuse contributions in the positions expected for the ordered phase. Similar patterns were obtained by heating individual fragments of the ordered form

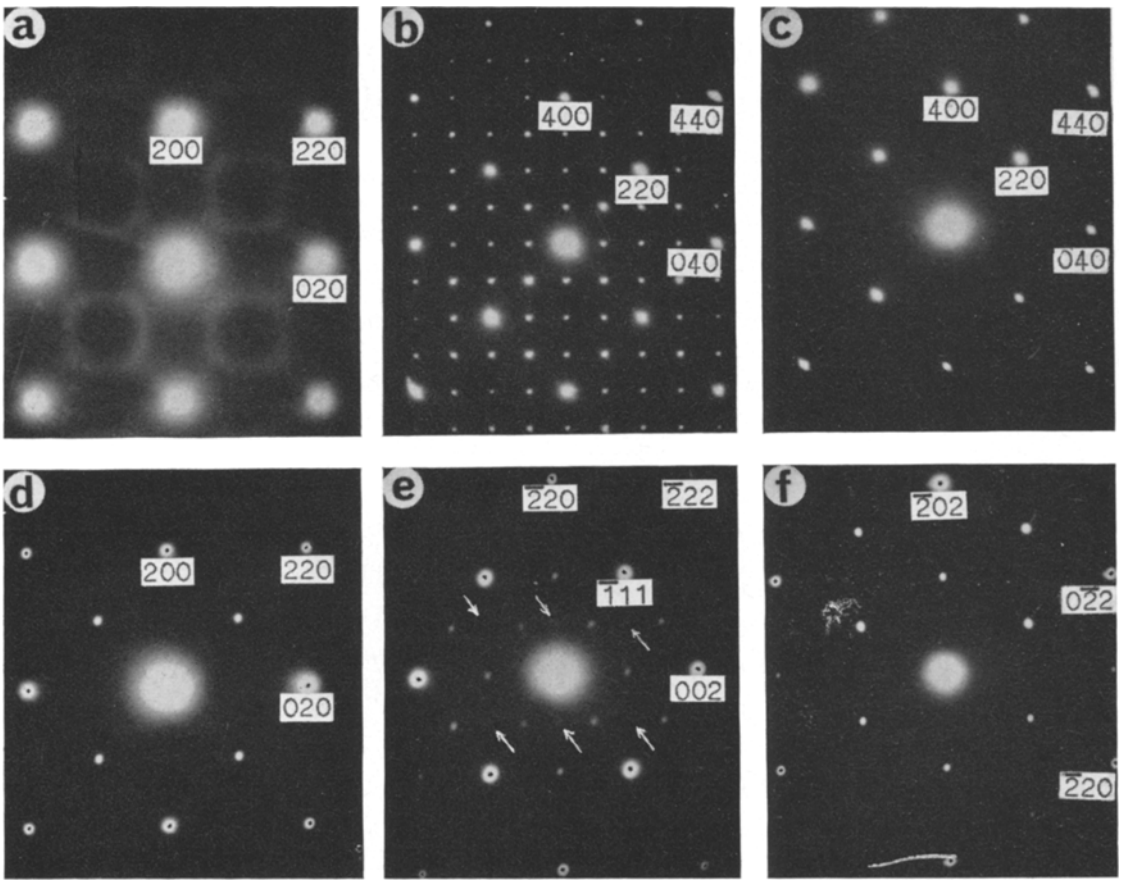

Figure 1 Electron diffraction patterns, showing particular reciprocal lattice sections of (a) pure α-$LiFeO_2$ (001). Note the diffuse scattering due to short range order of Li^+ and Fe^{3+}. (b) pure ordered $LiFe_5O_8$ (001). (c) pure disordered $LiFe_5O_8$ (001). (d) α-$LiFeO_2$, heated at 1000° C for 65 h, quenched in air (001). (e) α-$LiFeO_2$, heated at 1000° C for 65 h, annealed at 600° C (110). (f) α-$LiFeO_2$, heated at 1100° C for 65 h, quenched in air (111). Similar patterns were obtained from (111) fragments treated as in (d). Reflections due to α-$LiFeO_2$ in (d), (e), and (f) are marked with a black dot, and some of them are indexed. The remainder come from precipitates. Weak reflections in (e), marked by arrows, indicate that in this case, the precipitate is ordered. These patterns also contained diffuse scattering, which is not easily seen in the prints.

in the electron microscope, using a focused electron beam. Very rapid quenching was achieved by suddenly defocusing the beam. The as-prepared sample of $LiFe_5O_8$, which was cooled from 1100° C in air, was partly ordered; the spots unique to the space group $P4_332$ were sharp, but much less intense than those in fig. 1b.

The arrangement of the cations in both forms of $LiFe_5O_8$ is such that three-fifths of the Fe^{3+} and all the Li^+ ions occupy octahedral sites, and the remaining Fe^{3+} ions lie in tetrahedral sites of the spinel-type lattice. In the disordered form, the distribution of octahedral Fe^{3+} and Li^+ is random, and the ordering process involves a rearrangement of these cations so that each Li^+ is surrounded only by Fe^{3+} nearest neighbour cations [5]. As a consequence, the symmetry is lowered from face-centred to primitive, but the size of the unit cell is virtually unaltered (table I).

3.2. Decomposition of α-$LiFeO_2$, 1000° C for 65 h

A sample of α-$LiFeO_2$ was heated in air at 1000° C for 65 h. Electron diffraction patterns from fragments of the product (figs. 1d-f) contained weak foreign reflections in addition to the strong pattern from α-$LiFeO_2$. Dark field imaging using these reflections showed that they came from a coherent precipitate, whose appearance was strongly influenced by the thermal history of

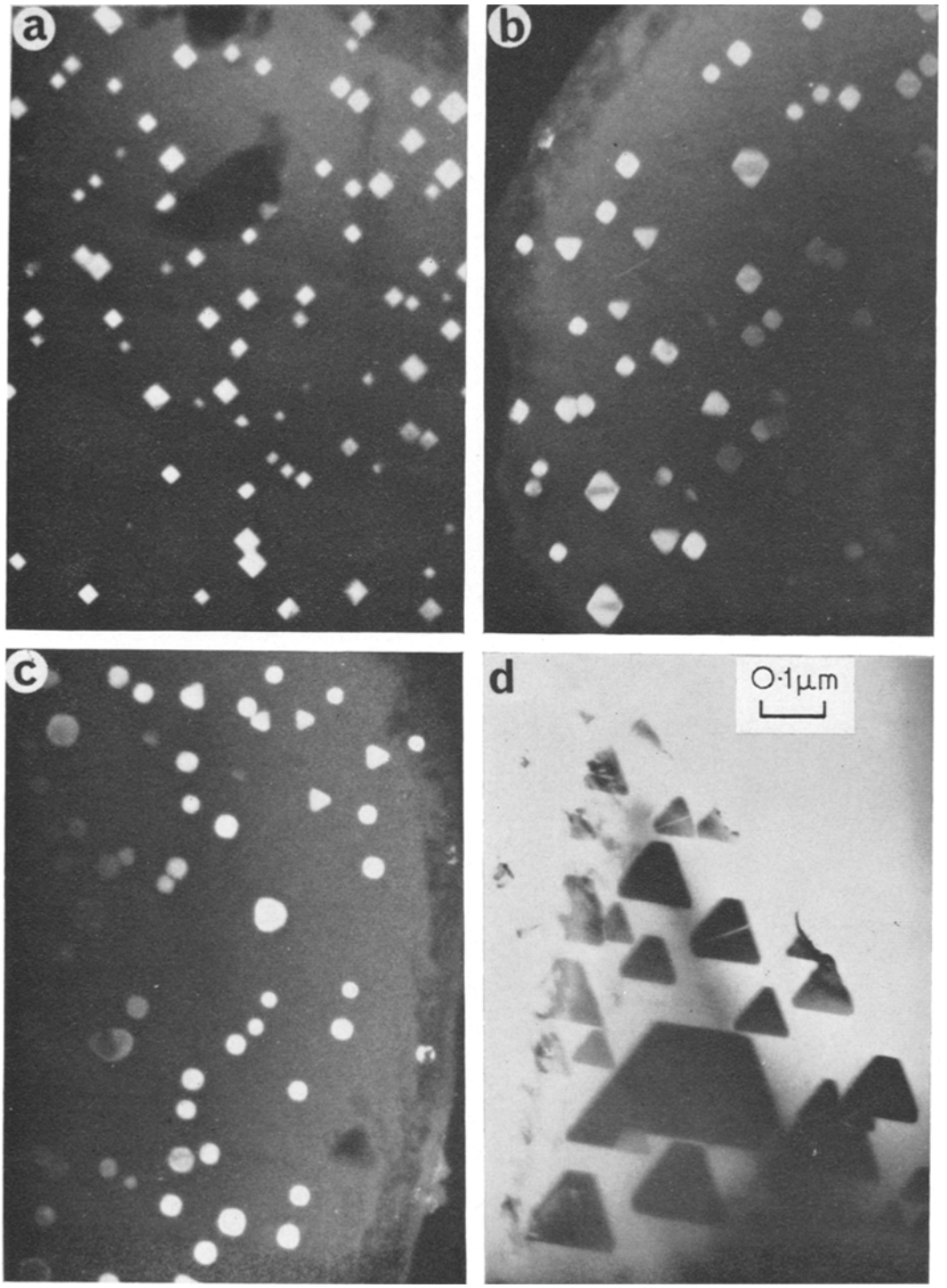

Figure 2 Images of precipitate particles in α-$LiFeO_2$ heated at 1000°C for 65 h, then annealed at 600°C. (a) (001), dark field. (b) (110), dark field. (c) (111), dark field. (d) (111), bright field. Some of the dark triangular precipitate particles contain white lines parallel to ⟨211⟩.

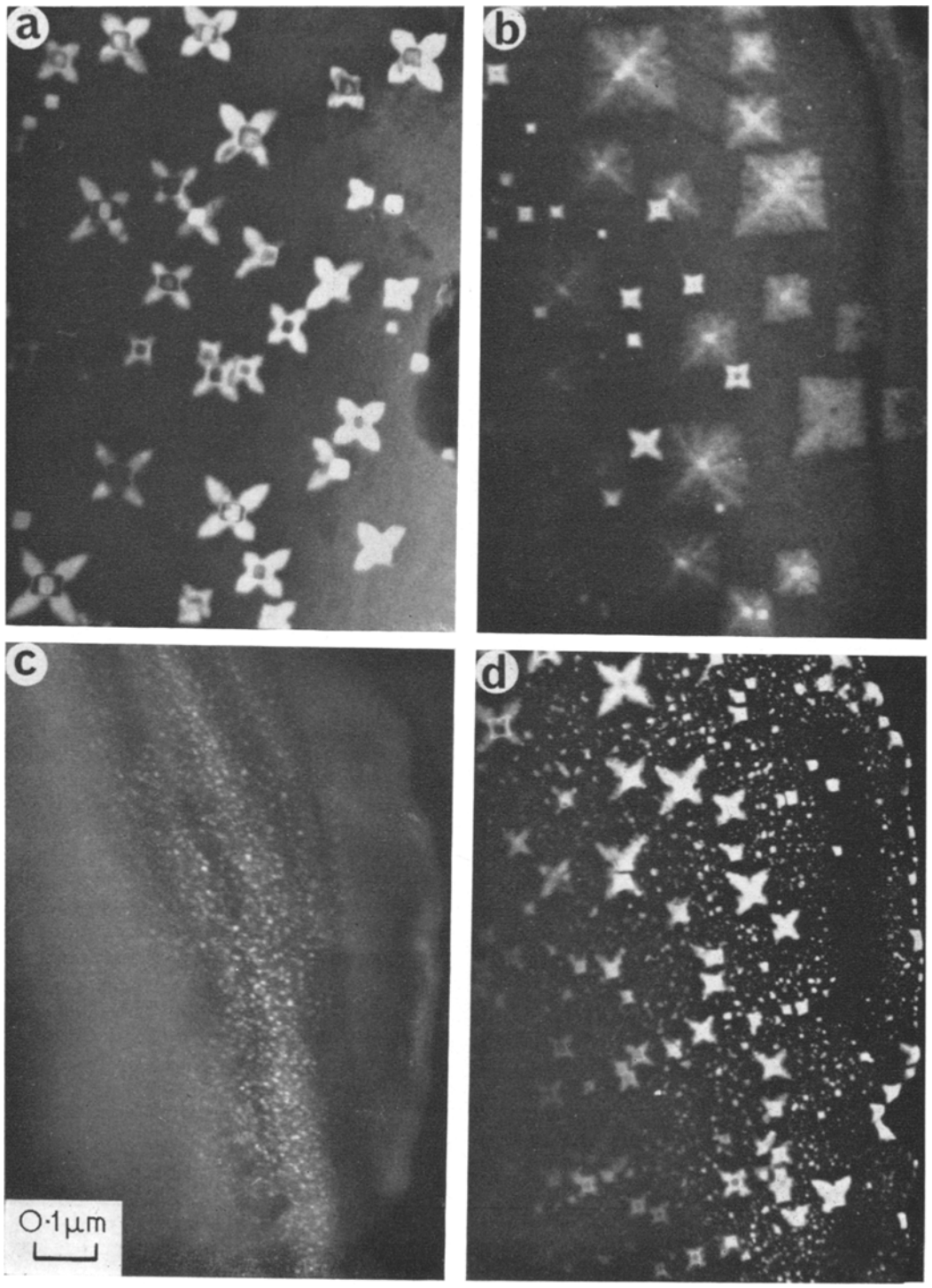

Figure 3 Dark field images of precipitate particles in α-$LiFeO_2$ heated at 1000°C for 65 h, then quenched. (a) Quenched in air (001). (b) Quenched in air (001). (c) Same area as (b), after electron beam heating and slow quenching by defocusing the beam. (d). Same area as (b), treated as for (c), but quenched more slowly.

the product subsequent to the treatment at 1000° C. Fig. 2 shows images of particles in a sample which had been annealed at 600°C for 18 h. The particles possess distinctive outlines depending upon orientation – square in (001) (fig. 2a), rhombic or triangular in (110) (fig. 2b), and hexagonal or triangular in (111) (figs. 2c and d). The indices refer to the planes in the matrix which lay perpendicular to the incident electron beam in each orientation. These outlines indicate that the majority of precipitate particles are octahedra, with their body-diagonals parallel to $\langle 100 \rangle_m$ directions (m = matrix of α-$LiFeO_2$), and the remainder are tetrahedra. All the particles have triangular faces coherent with the matrix on $\{111\}_m$ planes, and some of them, particularly those in fig. 2d, are severely truncated. Bright field images (e.g. fig. 2d) showed no signs of strain in the matrix in the neighbourhood of the precipitate particles.

Samples which were quenched from 1000°C in air contained star-shaped particles, oriented with their points along $\langle 100 \rangle_m$ (figs. 3a and b). Less frequently, precipitates having a dendritic appearance were observed (fig. 3b). This dendritic growth was barely visible in bright field, and probably occurs as very thin filaments on $\{111\}_m$ planes.

When samples were quenched from 1000°C into water, neither the precipitate nor its diffraction pattern was observed. The same effect was obtained by heating fragments in the electron beam of the microscope, and quenching by sudden defocusing. Precipitation could be induced by slowly defocusing the electron beam incident on a hot fragment. Figs. 3c and d are images of the same area as fig. 3b, recorded after heating and cooling the fragment several times by this means. The size of the particles obtained depended on the rate of cooling, which was faster prior to fig. 3c than fig. 3d. The quenching conditions in these *in situ* experiments were not determined, since the cooling rates could not be reproduced accurately, and they varied with the size of the fragment being examined and the conditions of illumination.

3.3. Decomposition of α-$LiFeO_2$, 1100°C for 65 h

A further period of heating for 65 h at 1100°C was accompanied by a significant loss in weight (*c.* 9%), and the X-ray powder diffraction pattern of the product indicated the presence of a second phase. The extra reflections were those expected for $LiFe_5O_8$. Electron diffraction patterns from individual fragments confirmed the presence of partly ordered $LiFe_5O_8$. Other fragments in the product gave patterns similar to those in figs. 1d-f, but dark field images showed that the precipitate grains were much larger than in figs. 2 and 3, and no longer possessed distinctive shapes (fig. 4).

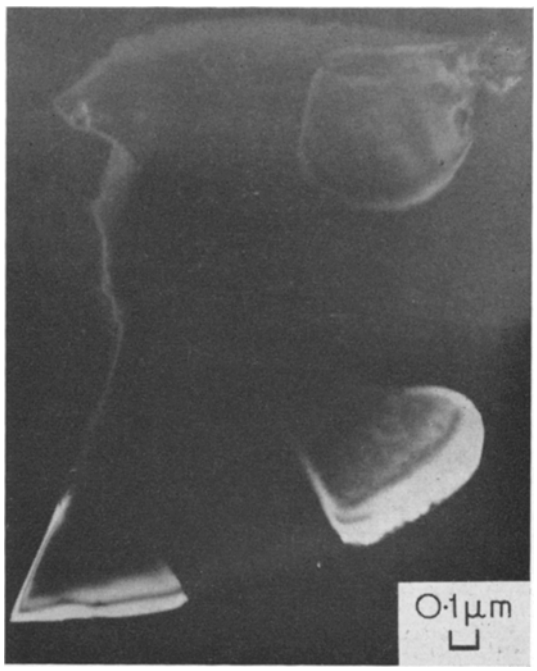

Figure 4 Dark field image, showing three large precipitate grains in a matrix of α-$LiFeO_2$, after heating at 1100°C for 65 h.

4. Discussion

The loss in weight of $LiFeO_2$ when it is heated at 1100°C is undoubtedly due to the volatilisation of lithium, probably as oxide. It appears that at high temperatures, a considerable loss of lithium can be tolerated by the NaCl-type lattice of α-$LiFeO_2$, and that this situation can be retained at lower temperatures by rapid quenching. However, precipitation occurs when the samples are cooled more slowly. The extra reflections due to the precipitate (figs. 1d-f) occur in positions expected for $LiFe_5O_8$. Since the arrangement of anions in the ideal spinel and rocksalt lattices are identical, and the unit cell dimensions of $LiFe_5O_8$ are almost exactly twice those of α-$LiFeO_2$ (table I), the precipitate can be accommodated in the matrix with negligible strain. Its formation

merely involves a redistribution of the cations over the available octahedral and tetrahedral sites. The ordered form of $LiFe_5O_8$ seemed less likely to appear as a precipitate, because the anions are slightly displaced from their spinel positions in this structure [5], and the consequent increase in strain energy at the interface with α-$LiFeO_2$ may outweigh the energy advantage gained by ordering at low temperatures. This prediction was partly confirmed by the observation that in the sample heated at 1100°C (section 3.3), separate fragments of $LiFe_5O_8$ were partly ordered, but precipitate grains such as are shown in fig. 4 were disordered. However, diffraction patterns from the sample heated at 1000°C and annealed at 600°C (e.g. fig. 1f) contained extra reflections (arrowed in fig. 1e) typical of ordered $LiFe_5O_8$. Thus it seems that in the precipitated $LiFe_5O_8$, the ordering transition is hindered, but not eliminated. It is of interest to note that some of the larger particles in the annealed samples (e.g. fig. 2d) contained defects, which appeared as white lines in bright field, parallel to $\langle 2\,1\,1 \rangle$. These are very probably antiphase boundaries, separating ordered domains of $LiFe_5O_8$.

The octahedral shape of the precipitate particles after annealing (fig. 2) is probably one of minimum interfacial energy, and is the same as the shape of macroscopic crystals of many spinels. Precipitates of $Mg_{1.2}Fe_{1.8}O_{3.9}$ in Fe^{3+}-doped MgO [7] also have octahedral shapes. The star-shaped and dendritic particles in fig. 3 were produced under conditions well removed from equilibrium, and are similar to the shapes obtained during crystallisation from solutions and melts, when the supersaturation is increased rapidly. The size and detailed geometry of the particles is clearly a sensitive function of the rate of cooling of the sample. The compact octahedra in fig. 2 probably contain as much material as the more open shapes in figs. 3a and b, which appear to be much larger. The latter may well collapse to octahedra by cation diffusion during annealing.

For fragments heat treated in the electron beam, as in figs. 3c and d, the rate of cooling will depend on the shape of the fragment, thin edges should cool more rapidly than thick regions. This may be the reason why the amount of precipitate in fig. 3d appears to be considerably greater than that in the same area prior to beam heating (fig. 3b). The micrographs show only the thinnest area of a much larger fragment, which would be the first part to cool to the temperature where precipitation begins. Under these conditions, the remainder of the fragment might act as a source of material for the precipitate, and the amount present in the thin areas would be increased. All these qualitative observations indicate that the mobility of the cations in the close-packed cubic lattice of oxygen anions must be very high.

The results also provide a possible explanation for the fact that magnetic susceptibility measurements on $LiFeO_2$ [8, 9] have suffered from the presence of minute amounts of a ferrimagnetic impurity, assumed to be $LiFe_5O_8$, undetectable by X-ray powder diffraction. Small departures from stoichiometry in the samples used may well result in the formation of precipitates of ferrimagnetic $LiFe_5O_8$ unless the samples were quenched very rapidly from about 1000°C.

Acknowledgements

I am indebted to Mr M. A. O'Keefe for preparing some of the samples and taking the X-ray diffraction photographs, and to Dr J. V. Sanders and Dr L. M. Clareborough for helpful discussions.

References

1. M. E. FINE in "The Chemistry of Extended Defects in Non-metallic Solids" (L. Eyring and M. O'Keeffe, eds., North Holland, 1969).
2. K. N. WOODS and M. E. FINE, *J. Am. Ceram. Soc.* **52**, (1969) 186.
3. E. POSNJAK and T. BARTH, *Phys. Rev.* **38** (1931) 2234.
4. A. HOFFMANN, *Naturwiss.* **26** (1938) 431.
5. P. B. BRAUN, *Nature* **170** (1952) 1123.
6. M. BRUNEL and F. DE BERGEVIN, *J. Phys. Chem. Solids* **30** (1969) 2011.
7. G. P. WIRTZ and M. E. FINE, *J. Am. Ceram. Soc.* **51** (1968) 402.
8. D. E. COX, G. SHIRANE, P. A. FLINN, S. L. RUBY, and W. J. TAKEI, *Phys. Rev.* **132** (1963) 1547.
9. J. C. ANDERSON, S. K. DEY, and V. HALPERN, *J. Phys. Chem. Solids* **26** (1965) 1555.

Received 23 November and accepted 28 December 1970.